JOURNAL OF GUIDANCE, CONTROL, AND DYNAMICS
Vol. 31, No. 5, September–October 2008

New Results on Linear Time Invariant and Parameter Varying Static Output Feedback

Ricardo S. Sánchez-Peña*
Institució Catalana de Recerca i Estudis Avançats and Universitat Politècnica de Catalunya, 08222 Barcelona, Spain
and
Phalguna Kumar Rachinayani† and Darío Baldelli‡
Zona Technology Inc., Scottsdale, Arizona 85258

DOI: 10.2514/1.34871

The increasing complexity of models related to future generation aircraft systems has encouraged the usage of linear parameter varying methodology with gain-scheduling control system configurations. This work presents new results on the design of static output feedback controllers by extending the $\mathcal{H}_\infty$ loop-shaping procedure to linear parameter varying models. In addition, an improved robustness measure is computed for both linear time invariant and linear parameter varying models. Extra constraints that guarantee closed-loop pole placement and a restricted structure for the static controller can also be imposed. Very promising results are illustrated by controller designs for both the lateral–directional and longitudinal dynamics of the F-16 aircraft.

I. Introduction

LINEAR parameter varying (LPV) models have become very popular as a means of describing a large class of nonlinear systems, with the possibility of using convex optimization for controller synthesis [1–3]. Most of the complex control problems in aerospace applications involve inner and outer feedback loops along with weighting functions and constant controller gains. The increasing complexity of models related to future generation aircraft systems has encouraged the usage of LPV methodology with gain-scheduling control system configurations. In particular, morphing aircraft conceived as multirole platforms that modify their external shape to adapt to changing environments are an important potential application. Dynamic models for morphing vehicles must properly take into account their inherent time-varying nature due to the dynamic coupling between inertial (wing's area and mass distribution changes), aerodynamic, structural, and distributed control forces. The time-varying aerodynamic forces and moments depend on the wing's shape changes due to the morphing command. One possible approach is to assume that the time-varying dynamics could be represented by an LPV plant model that approximately captures this complex behavior. The authors have presented preliminary results in this area in Baldelli et al. [4] using dynamic LPV controllers and reduced order controllers.

On the other hand, static output feedback (SOF) control design is an open nondeterministic polynomial time (NP) hard problem [5]. In recent years, this problem has been applied to aircraft systems [6] being reformulated as either a convex optimization problem using linear matrix inequalities (LMIs) or a nonconvex optimization problem to be solved by using nonlinear optimization methods [7]. The advantage provided by these controllers is their ease of implementation by a simple modification of the constant gains.

In the recent literature, classical robust $\mathcal{H}_\infty$-based control methodologies were applied to design SOF controllers for aircraft systems [8–10]. Most SOF designs require an initial stabilizing gain and the solution of three coupled equations: two Ricatti and a spectral radius condition. In Gadewadikar et al. [8], the authors provide both necessary and sufficient conditions for the existence of an $\mathcal{H}_\infty$ SOF controller in terms of only two coupled matrix equations: an LMI and one Ricatti equation. They extend this result to find all stabilizing static state-feedback controllers and solve the SOF $\mathcal{H}_\infty$ controller in terms of a single Ricatti equation and a free matrix parameter.

The loop-shaping $\mathcal{H}_\infty$ procedure [11] extensively used in aeronautics has several advantages. First, it produces a precomputable stability margin that may be related to simultaneous phase and gain margins in all input/outputs and computed using the gap metric and ν gap [12]. Second, it allows classical weight selection and loop-shaping methodologies to be used in the design process. And finally, the uncertainty set of models may include unstable ones. All these reasons make it especially attractive for aeronautical applications, particularly if static controllers may be synthesized. To this end, in Prempain and Postlethwaite [10], a sufficient condition in terms of two coupled LMIs is presented for this type of controllers when restricted to the case of SOF. This sufficient condition is used to design a loop-shaping $\mathcal{H}_\infty$ controller and applied to a Bell 205 research helicopter.

All the previous results on $\mathcal{H}_\infty$ SOF controllers [8–10] are derived for linear time invariant (LTI) models. In this paper, we extend the work of Prempain and Postlethwaite [10] and solve for both necessary and sufficient conditions to design a loop-shaping $\mathcal{H}_\infty$ SOF controller in terms of a coupled LMI and an algebraic Ricatti inequality (ARI). We provide a simple iterative algorithm that improves the performance and robustness measure. The conditions to impose a given structure on the controller are also formulated as part of the optimization routine, which is particularly important in aeronautical applications. In addition, new results on designing $\mathcal{H}_\infty$ SOF controllers for LPV models are presented. The fast-dynamics problem [13], typical of LPV controller synthesis, is also addressed by imposing additional constraints on the LMI optimization solution. Closely related iterative algorithms have been presented in Skelton et al. [14] in the context of LTI fixed order and fixed controller structure problems, also known as *dual LMI optimization* nonconvex problems.

The work is organized as follows. Section II presents the necessary background to solve the problem. Section III presents the main results: an algorithmic solution to improve the performance and robustness of the SOF controller, a pole clustering constraint, and the extension of this $\mathcal{H}_\infty$ loop-shaping-based SOF to LPV systems.

Received 28 September 2007; revision received 7 March 2008; accepted for publication 7 March 2008.

*ICREA and Advanced Control Systems, Research Professor. Senior Member AIAA.
†Researcher.
‡Project Manager. Senior Member AIAA.

Section IV illustrates these results by applying them to the design of a static controller for the LTI lateral–directional wing leveler of the F-16 as well as a static LPV controller for the longitudinal dynamics of the same aircraft. Final conclusions and future research directions end the paper in Sec. V.

II. Background

In this section, we provide the results from McFarlane and Glover [11,15] for the robust stabilization controller design applied to a normalized coprime factor uncertain set of models. This is also known as the $\mathcal{H}_\infty$ loop-shaping control problem and will be the base of our work.

A set of models with coprime factor uncertainty can be represented as follows:

$$\mathcal{G} = \{(\tilde{M}_0 + \Delta_M)^{-1}(\tilde{N}_0 + \Delta_N) : [\Delta_M \;\; \Delta_N] \in \mathcal{H}_\infty, \|[\Delta_M \;\; \Delta_N]\|_\infty < \delta\}$$

where $\tilde{M}_0$ and $\tilde{N}_0$ are the normalized left coprime factorizations of $G_0(s) = \tilde{M}_0^{-1}\tilde{N}_0$, and δ is the upper bound of the coprime factor uncertainties $[\Delta_M, \Delta_N]$. The advantage of this uncertainty description is that the plants in $\mathcal{G}$ may have a different number of right-half-plane poles.

The $\mathcal{H}_\infty$ robust stabilization design procedure is as follows.

1) Shape the model by pre- and postfiltering to obtain the nominal open-loop frequency response. That is, two weighting functions, $W_1(s)$ and $W_2(s)$, are sought such that the open-loop transfer matrix,

$$G(s) = W_2(s)G_0(s)W_1(s) \tag{1}$$

presents a desirable shape according to performance specifications such as steady-state error and bandwidth. Here, the coprime factorization is $G(s) = \tilde{M}^{-1}\tilde{N}$ (see Fig. 1).

2) Compute the stability margin

$$b_{GK} = \sqrt{\|I - [\tilde{M} \quad \tilde{N}]\|_H^2}$$

for the augmented plant from step 1, where $\|\cdot\|_H$ is the Hankel singular value. If $b_{GK} < \delta$, an LTI controller exists that stabilizes all models in $\mathcal{G}$ and fulfils the performance specifications. Otherwise, return to step 1 and modify the weighting functions until the robust stability condition is satisfied.

Here, the model of the augmented plant $G(s)$ has the following state-space representation:

$$G(s) \equiv \left[\begin{array}{cc} A & B \\ C & D \end{array}\right] \equiv \begin{cases} \dot{x}(t) = Ax(t) + Bu(t) \\ y(t) = Cx(t) + Du(t) \end{cases} \tag{2}$$

The design problem to be solved is posed as a combination of performance and robustness, the latter in terms of a family of models with coprime factor uncertainty (see Fig. 1):

$$\left\| \left[\begin{array}{c} K(s) \\ I \end{array}\right] [I + G(s)K(s)]^{-1}\tilde{M}^{-1}(s) \right\|_\infty < \gamma \tag{3}$$

where $G(s) = \tilde{M}^{-1}\tilde{N}$ is the left coprime factorization of the (augmented) model. The solution to the aforementioned $\mathcal{H}_\infty$ robust stabilization problem is an LTI controller, $K(s)$ (also known as a central controller), whereas, for the SOF problem, the controller search is carried out over constant Ks.

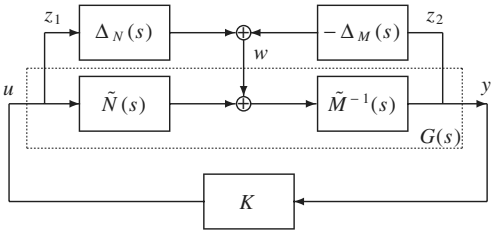

Fig. 1 Design problem setup.

The following result [10] provides a sufficient condition to design an $\mathcal{H}_\infty$ loop-shaping-based SOF controller for the previous (augmented) model in Eq. (2):

Theorem 1: Let $L = -(BD^T + ZC^T)E^{-1}$, $F = (I + D^TD)$ and $E = (I + DD^T)$, where $Z \geq 0$ satisfies the algebraic Ricatti equation:

$$\begin{aligned}(A - BF^{-1}D^TC)Z + Z(A - BF^{-1}D^TC)^T \\ - ZC^TE^{-1}CZ + BF^{-1}B^T = 0\end{aligned} \tag{4}$$

A static controller K which satisfies Eq. (3) can be computed if there exists a matrix $R > 0$ and a scalar $\gamma > 1$ solving the inequalities

$$(A + LC)R + R(A + LC)^T < 0 \tag{5}$$

$$\left[\begin{array}{ccc} AR + RA^T - \gamma BB^T & RC^T - \gamma BD^T & -L\sqrt{E} \\ CR - \gamma DB^T & -\gamma E & \sqrt{E} \\ -\sqrt{E}L^T & \sqrt{E} & -\gamma I_{n_y} \end{array}\right] < 0 \tag{6}$$

where $\sqrt{E}$ represents $E^{1/2}$, for simplicity.

Inserting the previous result, (γ, R), in the following LMI equation and solving for $\tilde{K}$ yields

$$\left[\begin{array}{ccc} A_{cl}R + RA_{cl}^T & RC_{cl}^T & B_{cl} \\ C_{cl}R & -\gamma I & D_{cl} \\ B_{cl}^T & D_{cl}^T & -\gamma I \end{array}\right] < 0 \tag{7}$$

$$\begin{cases} A_{cl} = A + B\tilde{K}C, & B_{cl} = (B\tilde{K} - L)\sqrt{E} \\ C_{cl} = \left[\begin{array}{c} \tilde{K} \\ I + D\tilde{K} \end{array}\right]C, & D_{cl} = \left[\begin{array}{c} \tilde{K} \\ I + D\tilde{K} \end{array}\right]\sqrt{E} \end{cases} \tag{8}$$

where a static controller, K, can be obtained as follows: $K = -\tilde{K}(I + D\tilde{K})^{-1}$. □

In the same work [10], a necessary and sufficient condition for the previous result can be obtained if Eq. (5) is replaced by the more restrictive ARI:

$$(A + LC)R + R(A + LC)^T - \gamma RC^TE^{-1}CR < 0 \tag{9}$$

The values of (γ, R), which solve this equivalent condition together with Eq. (6), belong to the feasible set that contains the optimal value of γ. Here, we find a $\gamma_\star$ in this set, which improves previous results [10].

III. Main Results

Based on Theorem 1, we point out some extensions that will be performed in this section:

1) The conditions presented in the previous result are only sufficient, and an improved solution, that is, lower γ, can be obtained by iteratively solving the necessary and sufficient conditions, Eqs. (6) and (9). In the case of $D = 0$, then $K = -\tilde{K}$ and a structure can be imposed onto the controller K as part of the LMI optimization.

2) An additional closed-loop pole placement LMI provides an extra tool to shape the time response of the closed-loop system and fits the LMI formulation of the problem. In the case of LPV systems, it is very useful in eliminating the "fast poles" phenomenon [13].

3) Matrix L need not be the stabilizing solution of the normalized coprime factors of the shaped model $G(s)$, just one that stabilizes any set of coprime factors of $G(s)$. This eliminates the need to solve an extra Ricatti or LMI equation to find the stabilizing solution for the normalization of the coprime factors. This is instrumental in extending all previous results to LPV systems.

A. Improved Bounds on γ

The equations that provide the analysis and synthesis tools to obtain an optimal SOF $\mathcal{H}_\infty$ loop-shaping controller are Eqs. (6), (7), and (9) in the variables $(\gamma, R, \tilde{K})$. These represent an ARI and two

LMIs, which produce a nonconvex optimization problem. Here, we present an algorithmic procedure that iteratively improves the performance and robustness measure γ, that is, we compute a better bound $\gamma_\star \le \gamma$.

The procedure in Prempain and Postlethwaite [10] solves the LMIs (5) and (6) to obtain (γ, R). These are sufficient conditions that produce an upper bound for the optimal γ, denoted as $\gamma_{\max} \stackrel{\Delta}{=} \gamma^0_{\max}$, and also $R_{\max}$. Furthermore, due to the fact that Eqs. (6), (7), and (9) are necessary and sufficient conditions to solve the design problem in $(\gamma, R, \tilde{K})$, solving only Eq. (6) or Eq. (7) provides the necessary conditions that produce a lower bound $\gamma_{\min} \stackrel{\Delta}{=} \gamma^0_{\min}$ as well as $R_{\min}$.

At the ith iteration and by using a convex combination of both bounds,

$$\begin{aligned} \gamma &= (1-\lambda)\gamma^i_{\min} + \lambda\gamma^i_{\max} = f(\lambda), \\ R &= (1-\lambda)R_{\min} + \lambda R_{\max} = g(\lambda), \qquad \lambda \in [0,1] \end{aligned} \tag{10}$$

we obtain linear functions of λ. The algorithm to compute the value $\gamma_\star \in [\gamma^N_{\min}, \gamma^N_{\max}]$ is as follows:

Algorithm 1

Step 1: Replace $\gamma = f(\lambda)$ and $R = g(\lambda)$ in Eqs. (6) and (9) and solve

$$\lambda_1 = \min\{\lambda \text{ such that Eqs. (6), (9) hold}\}$$

Compute $\gamma_1 = f(\lambda_1)$ and $R_1 = g(\lambda_1)$.

Step 2: Replace (γ_1, R_1) in Eq. (7) and solve for $\tilde{K}$.

IF $\gamma_1 = \gamma_{\max}$, the sufficient ($\Rightarrow$) and equivalent ($\Leftrightarrow$) conditions coincide, $\gamma_\star = \gamma_1$ and STOP (only for the first iteration $i = 0$).

Step 3: Replace $\tilde{K}$ in Eq. (7) and find

$$\gamma_2 = \min\{\gamma \text{ such that (7) holds } R_2 = R > 0\}$$

IF $|\gamma_1 - \gamma_2| < \epsilon$, OR iteration $i = N$, $\gamma_\star = \gamma_1$ and STOP.[§]

ELSE $i \to i+1$ and replace $\gamma^i_{\max} = \gamma_1$, $R_{\max} = R_1$, $\gamma^i_{\min} = \max(\gamma^{i-1}_{\min}, \gamma_2)$, and $R_{\min} = R_2$ in Eqs. (10), and

GO TO step 1.

Step 1 computes a lower $\gamma_1 \le \gamma^i_{\max}$ that meets the equivalent conditions (6) and (9) and provides the upper bound for the next iteration. Step 2 computes the corresponding controller $\tilde{K}$, which is further verified in step 3 through the synthesis condition (7), and again a minimum γ is computed. The outcome of this last step, γ_2, is compared with the previous lower bound $\gamma^{i-1}_{\min}$. The larger one is the new lower bound for the next iteration of the λ search in step 1. Note that (γ_2, R_2) need not satisfy Eqs. (6) and (9). Therefore, a lower value $\gamma_\star$ will be reached as the converging point of the *upper* bound sequence. The procedure stops when either the upper and lower bounds are within an interval of size ϵ or the last (Nth) iteration has been reached. The result is stated formally as follows.

Lemma 1: Algorithm 1 converges to a suboptimal improved solution, $\gamma_\star = \gamma^N_{\max} \ge \gamma^N_{\min}$, which together with an $R > 0$ and a static controller $\tilde{K}$ satisfies Eqs. (6), (7), and (9).

Proof: There exists a value $\gamma_\star$ in the interval $\gamma_{\max} \ge \gamma_\star \ge \gamma_{\min}$ that, for a given $R > 0$, satisfies both necessary and sufficient inequalities (6) and (9) as well as the synthesis Eq. (7). (Here we do not claim we reach the optimal, but only a better (lower) solution for γ.) It is clear that the minimal γ that achieves both sufficient conditions (5) and (6) provides an initial upper bound $\gamma^0_{\max}$. In step 1 and for the ith iteration, the minimization to the value $\gamma^i_1 \le \gamma^i_{\max}$ provides the next upper bound, that is, $\gamma^{i+1}_{\max} \le \gamma^i_{\max}$.

The minimal γ that achieves only the necessary condition (6) produces an initial lower bound $\gamma^0_{\min}$ for the solution. At the ith iteration, once a controller $\tilde{K}$ has been found, the synthesis equation (7) also provides a lower bound. In step 3, the new lower bound is obtained as the larger of the two; hence, $\gamma^i_{\min} \le \gamma^{i+1}_{\min}$. In addition, $\gamma^0_{\min} \le \gamma^i_{\max}$ and, because $\{\gamma^i_{\max}\}$ is a monotonically decreasing sequence, it converges to a value $\gamma_\star$.

[§]Another possible stopping criterion is when a small increment, ϵ_{iter}, between iterations is reached, that is, $|\gamma^i_{\max} - \gamma^{i-1}_{\max}| < \epsilon_{\text{iter}}$.

At the ith iteration in steps 2 and 3, the same Eq. (7) is solved and the same value $\tilde{K}$ is used. Because γ is minimized in step 3, then $\gamma^i_2 \le \gamma^i_1$. As a consequence of all the previous arguments,

$$\gamma^0_{\min} \le \cdots \le \gamma^i_{\min} \le \gamma^{i+1}_{\min} \le \cdots \le \gamma_\star \le \cdots \le \gamma^{i+1}_{\max} \le \gamma^i_{\max} \cdots \le \gamma^0_{\max}$$

and the upper bound approaches the value $\gamma_\star$. At the last (from a computational point of view) iteration $i = N$, for the resulting value $\gamma_\star = \gamma^N_{\max}$ there is an $R > 0$ and a controller $\tilde{K}$ that satisfy Eqs. (6), (7), and (9). The lower bound $\gamma^N_{\min} \le \gamma_\star$ provides a way to test how good the suboptimal value $\gamma_\star$ is. The algorithm stops if it is within a given ϵ neighborhood of the upper bound or if a prescribed maximum iteration N is reached. Another possible stopping criteria is when a small increment ϵ_{iter} between iterations is reached, that is, $|\gamma^i_{\max} - \gamma^{i-1}_{\max}| < \epsilon_{\text{iter}}$. □

In the case $D \equiv 0$, as in most physical applications, $K = -\tilde{K}$, and when solving step 2 a particular structure can be assigned to $\tilde{K}$, for example, zeros in certain input–output channels. This is particularly useful in aeronautical applications in which classical controller structures are mostly used, as in the example in Sec. IV taken from [16,17].

Although a significant improvement has been presented here, the optimal solution to the SOF $\mathcal{H}_\infty$ loop-shaping problem requires further research. To this end, relations with similar iterative algorithms [14] to design fixed-order/fixed-structure controllers, known as *dual LMI optimization* nonconvex problems, could be explored.

B. Closed-Loop Pole Placement

From Chilali and Gahinet [18], we obtain extra LMIs that guarantee the closed-loop poles will be located in a particular region (see, for example, Fig. 2), which should be symmetric with respect to the real axis and are defined as follows.

Definition 1: A subset $\mathcal{D}$ of the complex plane is called an LMI region if there exist a symmetric matrix $\alpha = [\alpha_{k\ell}] \in \mathbb{R}^{m\times m}$ and a matrix $\beta = [\beta_{k\ell}] \in \mathbb{R}^{m\times m}$ such that $\mathcal{D} = \{z \in \mathbb{C}: f_{\mathcal{D}}(z) < 0\}$ with

$$f_{\mathcal{D}}(z) = \alpha + z\beta + \bar{z}\beta^T = [\alpha_{k\ell} + \beta_{k\ell} z + \beta_{\ell k}\bar{z}]_{1\le k,\ell\le m}$$

The result that guarantees the poles of the closed-loop system will be located in region $\mathcal{D}$ is presented next.

A matrix $A \in \mathbb{R}^{n\times n}$ is $\mathcal{D}$ stable if and only $\exists X > 0$:

$$\alpha_{k\ell} X + \beta_{k\ell} AX + \beta_{\ell k} XA^T < 0, \qquad 1 \le k, \ell \le m$$

These LMIs are included when solving step 2 as follows:

$$\alpha_{k\ell} R + \beta_{k\ell} A_{cl} R + \beta_{\ell k} R A^T_{cl} < 0, \qquad 1 \le k, \ell \le m$$

with $A_{cl} = A + B\tilde{K}C$.

C. Generalization to LPV Models

Given an LPV (augmented) model G_s, with $\rho = \rho(t)$ a time-varying parameter that takes values in the region $\mathcal{P}$,

$$G_s = \begin{bmatrix} A(\rho) & B(\rho) \\ C(\rho) & D(\rho) \end{bmatrix} \tag{11}$$

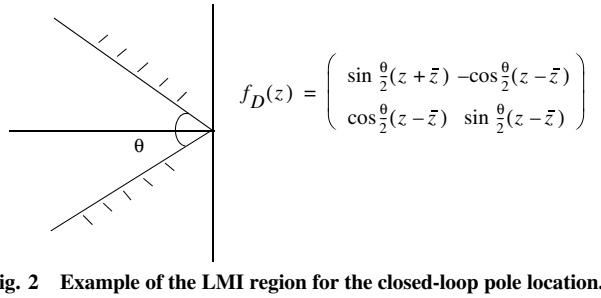

Fig. 2 Example of the LMI region for the closed-loop pole location.

Using the results in Xie and Eisaka [19,20], its (left) coprime factors, $G_s(\rho) = \tilde{M}^{-1}(\rho)\tilde{N}(\rho)$, can be computed as follows:

$$[\tilde{N}(\rho) \quad \tilde{M}(\rho)] = \begin{bmatrix} A(\rho)+L(\rho)C(\rho) & B(\rho)+L(\rho)D(\rho) & L(\rho) \\ E^{-\frac{1}{2}}(\rho)C(\rho) & E^{-\frac{1}{2}}(\rho)D(\rho) & E^{-\frac{1}{2}}(\rho) \end{bmatrix} \tag{12}$$

where $L(\rho)$ is such that $A_\ell(\rho) = A(\rho) + L(\rho)C(\rho)$ is parameter-dependent quadratically stable, that is, there exists a positive definite matrix $P(\rho)$ such that

$$A_\ell^T(\rho)P(\rho) + P(\rho)A_\ell(\rho) + \frac{\mathrm{d}P(\rho)}{\mathrm{d}t} < 0$$

This reduces to a simplified version if we select a constant P. Similar results can be obtained for the right coprime factors.

For SOF, $L(\rho)$ need not be the stabilizing solution of the *normalized* coprime factors of the augmented model G_s, but instead any coprime factors of G_s. The reason for this is that the complete development of the loop-shaping $\mathcal{H}_\infty$ controller can be done with any regular (left or right) coprime factors. The normalized coprime factors are useful only to determine beforehand the maximum coprime factor stability margin (see b_{GK} in Sec. II), which may be achieved when considering a general dynamic controller. In this case, due to the fact that the controller is static, this margin will not be achieved in general and, therefore, need not be precomputed, and the computational burden is thus reduced.

In any case, the normalized coprime factors can be computed [21] by applying *contractive* (left) normalized coprime factors. Here, the coprime factors can be computed from Eq. (12) with $L(\rho) = -(BD^T + ZY^{-1}C^T)E^{-1}$, where $Y > 0$ satisfies the following LMI:

$$\begin{bmatrix} \overbrace{Y(A - BF^{-1}D^TC)}^{H} + H^T - C^TE^{-1}C & YB \\ B^TY & -F^{-1} \end{bmatrix} < 0$$

This LMI can be derived by Schur complementing Eq. (4), after changing variables $Y = Z^{-1}$. Here, we have dropped the dependency with ρ for simplicity.

The procedure to design the controller for the LPV case follows the one for the LTI case of Theorem 1, with the additional consideration that the LMIs should be satisfied for all $\rho \in \mathcal{P}$. This will not be repeated here but amounts in general to an infinite number of LMIs that can be solved approximately by gridding the parameter variation region. Further controller analysis is needed to guarantee the quadratic stability and performance results. A common practice is to test the controller over a finer grid of the parameter variation region.

If, instead, we seek computable conditions, that is, a finite number of LMIs, the following more restrictive but practical result can be proved.

Lemma 2: Given an (augmented) LPV model $G_s(\rho)$ defined in Eq. (11), assume $A(\rho)$ depends affinely on $\rho(t)$, $B(\rho) = B$ and $D(\rho) = D$ are constant, and either 1) $C(\rho) = C$ is constant or 2) $C(\rho)$ depends affinely on $\rho(t)$.

Also assume region $\mathcal{P}$ is a convex polytope with vertices ρ_i, $i = 1, \ldots, m$ and the left coprime factors for $G_s(\rho)$ are computed as in Eq. (12) with L such that $A(\rho) + LC(\rho)$ is parameter-dependent quadratically stable. There exists a static 1) parameter-dependent controller $K(\rho)$ or 2) constant controller K that achieves the performance condition

$$\left\| \begin{bmatrix} y(t) \\ u(t) \end{bmatrix} \right\|_2 < \gamma \|w(t)\|_2$$

where $y(t) = K(\rho)[I + G_s(\rho)K(\rho)]^{-1}\tilde{M}^{-1}(\rho)w(t)$ and $u(t) = [I + G_s(\rho)K(\rho)]^{-1}\tilde{M}^{-1}(\rho)w(t)$, if there exists a matrix $R > 0$ and a scalar $\gamma > 1$ solving the inequalities

$$[A_i + LC_i]R + R[A_i + LC_i]^T < 0 \tag{13}$$

$$\begin{bmatrix} A_iR + RA_i^T - \gamma BB^T & RC_i^T - \gamma BD^T & -L\sqrt{E} \\ \star & -\gamma E & \sqrt{E} \\ \star & \star & -\gamma I_{n_y} \end{bmatrix} < 0 \tag{14}$$

(Here, systems are represented as LPV in state space, and the product among them is understood as their series connection. Also $K(\rho)$ is either a function of ρ in case 1 or constant as in case 2.) Here, $A_i = A(\rho_i)$ for all ρ_i, $i = 1, \ldots, m$ and either 1) $C_i = C$ or 2) $C_i = C(\rho_i)$. Also, $\star$ represents the elements that complete the symmetric matrix.

Proof: The proof follows the steps of Theorem 1 in Prempain and Postlethwaite [10], now for the LPV case. Considering that, under the previous assumptions, the time-varying parameter $\rho(t)$ appears affinely in both LMIs (13) and (14), only their extreme values ρ_i, $i = 1, \ldots, m$ need to be verified. □

In the more general case in which $B(\rho)$ and $D(\rho)$ are functions of the time-varying parameter, a simple solution is to dynamically filter the control input $\tilde{u} = W(s)u$. As a consequence, the ρ dependency is transferred to the new A and C matrices and the previous result can be applied [1].

To recover the LPV controller $K(\rho)$ using a finite set of LMIs, the following result holds.

Lemma 3: Let $\tilde{K}(\rho)$ be the solution to the following finite set of LMIs at the extreme values of the parameter variation set $\mathcal{P}$ in two cases: 1) C is constant and $\tilde{K}(\rho)$ varies affinely with $\rho(t)$ as in Eq. (15) and 2) $C(\rho)$ is affine in $\rho(t)$ and $\tilde{K}$ is constant as in Eq. (16):

$$\tilde{A}_i + \tilde{B}\,\tilde{K}\,\tilde{C}_i + [\tilde{B}\,\tilde{K}\,\tilde{C}_i]^T < 0, \qquad i = 1, \ldots, m \tag{15}$$

$$\tilde{A}_i + \tilde{B}\tilde{K}_i\tilde{C} + [\tilde{B}\tilde{K}_i\tilde{C}]^T < 0, \qquad i = 1, \ldots, m \tag{16}$$

with

$$\tilde{A}_i = \begin{bmatrix} A_iR + RA_i^T & 0 & RC_i^T & -L\sqrt{E} \\ 0 & -\gamma I_{n_u} & 0 & 0 \\ C_iR & 0 & -\gamma I_{n_y} & \sqrt{E} \\ -\sqrt{E}L^T & 0 & \sqrt{E} & -\gamma I_{n_y} \end{bmatrix},$$

$$\tilde{B} = \begin{bmatrix} B \\ I_{n_u} \\ D \\ 0 \end{bmatrix}, \qquad \tilde{C}_i = \begin{bmatrix} C_iR & 0 & 0 & \sqrt{E} \end{bmatrix}$$

Then the static LPV controller $K(\rho) = -\tilde{K}(\rho)[I + D\tilde{K}(\rho)]^{-1}$ solves the preceding performance problem.

Proof: Inserting (γ, R) from Lemma 2 in Eq. (7) and replacing A_{cl}, B_{cl}, C_{cl}, and D_{cl} as defined previously for the LTI case in Eq. (8), we obtain

$$\tilde{A}(\rho) + \tilde{B}\,\tilde{K}(\rho)\tilde{C}(\rho) + [\tilde{B}\,\tilde{K}(\rho)\tilde{C}(\rho)]^T < 0$$

which should be achieved for all $\rho \in \mathcal{P}$. To solve this with a finite set of LMIs, either $C(\rho)$ should be affine in $\rho(t)$ and $\tilde{K}$ constant or vice versa. In both cases, only the extreme values need to meet the inequalities, either at 1) $\tilde{A}(\rho_i) = \tilde{A}_i$ and $\tilde{C}(\rho_i) = \tilde{C}_i$ or 2) $\tilde{A}(\rho_i) = \tilde{A}_i$ and $\tilde{K}(\rho_i) = \tilde{K}_i$, which produces Eq. (15) or Eq. (16), respectively. The controller $K(\rho)$, either constant or time varying, is obtained from $\tilde{K}(\rho)$ according to Theorem 1.

In case 2, the controller is implemented as a convex combination of its extreme values $K(\rho_i) = K_i$, $i = 1, \ldots, m$ using the values of $\rho_m(t)$ measured in real time. At each time t, from

$$\rho_m = \sum_{i=1}^{m} \rho_i\lambda_i$$

under the restriction

$$\sum_{i=1}^{m} \lambda_i = 1$$

the set $\{\lambda_i, i = 1, \ldots, m\}$ is obtained and

$$K(\rho) = \sum_{i=1}^{m} K_i \lambda_i$$

is computed. □

Here, the affine LPV controller applies when only the dynamics are parameter dependent, whereas the constant static controller K solves a robust SOF problem that applies to the multimodel plant (A_i, B, C_i, D), for all $i = 1, \ldots, m$.

To obtain a lower value for the performance measure γ, the same algorithmic procedure from Sec. III can be applied to all vertices ρ_i, $i = 1, \ldots, m$ of the parameter variation region. A better performance and robustness will be achieved at the expense of extra computational work.

Because the $\mathcal{H}_\infty$ loop-shaping procedure produces a controller for an augmented model, $G_s(\rho)$, the plant weighting functions need to be restored to the controller to implement it. This increases the order slightly, depending on the order of the weights. The final controller is $\mathbf{K}[\rho(t)] = W_r(\rho)K(\rho)W_\ell(\rho)$, where $W_r(\rho)$ and $W_\ell(\rho)$ are the right and left weighting functions. In general, for stable weighting functions with state space representations,

$$W_\ell(s) = \begin{bmatrix} A_\ell & B_\ell \\ C_\ell & D_\ell \end{bmatrix}, \qquad W_r(s) = \begin{bmatrix} A_r & B_r \\ C_r & D_r \end{bmatrix}$$

and the final controller will have stable dynamics with the following state-space structure:

$$\mathbf{K}[\rho(t)] = \begin{bmatrix} A_k & B_k \\ C_k & D_k \end{bmatrix} \triangleq \begin{bmatrix} A_\ell & 0 & B_\ell \\ B_r K(\rho) C_\ell & A_r & B_r K(\rho) D_\ell \\ D_r K(\rho) C_\ell & C_r & D_r K(\rho) D_\ell \end{bmatrix}$$

This is due to the fact that, if the weights are stable, there exist $P_1 > 0$ and $P_2 > 0$ that satisfy the Lyapunov equations:

$$\left.\begin{aligned} A_\ell P_1 + P_1 A_\ell^T < 0 \\ A_r P_2 + P_2 A_r^T < 0 \end{aligned}\right\} \Rightarrow A_k \begin{bmatrix} P_1 & 0 \\ 0 & P_2 \end{bmatrix} + \begin{bmatrix} P_1 & 0 \\ 0 & P_2 \end{bmatrix} \qquad A_k^T < 0$$

Note that stability can be proved using a single Lyapunov function (independent of the time-varying parameter $\rho(t)$). (This can be proved by applying the Schur complement to the right-hand side Lyapunov equation.) The fact that the eigenvalues of A_k only depend on the weight dynamics (A_r, A_ℓ) is not enough to prove this result because the system is time varying.

As a future research issue, a computable static LPV controller for more general plant models could be pursued using full block multipliers [3].

IV. Examples

The approach proposed in this work will be applied to two different case studies taken from Stevens and Lewis [17] on the F-16 aircraft. Both cases represent typical design scenarios that a flight control designer usually faces, that is, a predefined controller topology with inner/outer loops, integrators and washout filters allowed only on either of the loops, and very few gains to be estimated/computed. Additionally, gain scheduling throughout the altitude and Mach/airspeed parameters within the operational flight envelope of the air vehicle must be accomplished.

The first example involves the design of a lateral–directional (LTI) multi-input/multi-output (MIMO) controller to keep the air vehicle's wing leveled while washing out any yaw rate, r_w, that has built up due to the Dutch roll mode. The second case study involves the design of a multiloop (LPV) longitudinal dynamics controller for which the gain coefficients are automatically gain scheduled as a function of the altitude and true airspeed while the vehicle is performing a very aggressive pitch-up maneuver. In both cases, the values of γ are not normalized to 1; hence, the best (lower) value is computed, which could be larger than 1. Otherwise, the weighting functions should be modified until $\gamma_\star = 1$ is achieved.

A. LTI Case: Wing-Leveler Control

By using the example presented in Kureemun and Bates [16] and Stevens and Lewis [17] (see Fig. 3 for the block diagram), the lateral–directional MIMO control system for the F-16 aircraft was designed using the method mentioned in Algorithm 1. Here, we present three different designs, depending on the performance specifications. The system matrices are presented in the Appendix.

1) In this first design, the open-loop (input) weighting function, $W_{\text{in}}(s)$, equal to the one in Kureemun and Bates [16], and the static fixed structure controller K_1 are as follows:

$$W_{\text{in}}(s) = \text{diag}[\, W_{e_\phi} \quad W_{e_r}\,] = \begin{bmatrix} \frac{1}{s} & 0 \\ 0 & 1 \end{bmatrix},$$

$$K_1 = \begin{bmatrix} 0.986 & 0 & -1.0769 & 3.99 \\ 0 & 0.542 & 0 & 0 \end{bmatrix}$$

The response, which is slightly slower than the one in Kureemun and Bates [16] obtained by an optimization method, is illustrated in Fig. 4. The reason is that our design reaches the (sub)optimal $\gamma_\star = 4.9$, which optimizes the robustness against coprime factor uncertainty. In this case, the sufficient condition computed by the method in Prempain and Postlethwaite [10] produces $\gamma_{\max} = 9.91$. Therefore, the main effort has been made to improve the robustness instead of the performance because the latter depends only on the weight. In the following designs, we change it to improve both the performance and the robustness.

2) More general input (W_{in}) and output (W_{out}) weights have been selected in this example, to improve the performance while optimizing the robustness against coprime factor uncertainty. The static fixed structure controller and the weights are as follows:

$$K_2 = \begin{bmatrix} 0.606 & 0 & -0.8123 & 1.0688 \\ 0 & 0.26806 & 0 & 0 \end{bmatrix},$$

$$W_{\text{in}}(s) = \begin{bmatrix} \frac{1}{s} & 0 \\ 0 & 1 \end{bmatrix}, \qquad W_{\text{out}}(s) = \text{diag}[\,25 \quad 0.1 \quad 10 \quad 22.5\,]$$

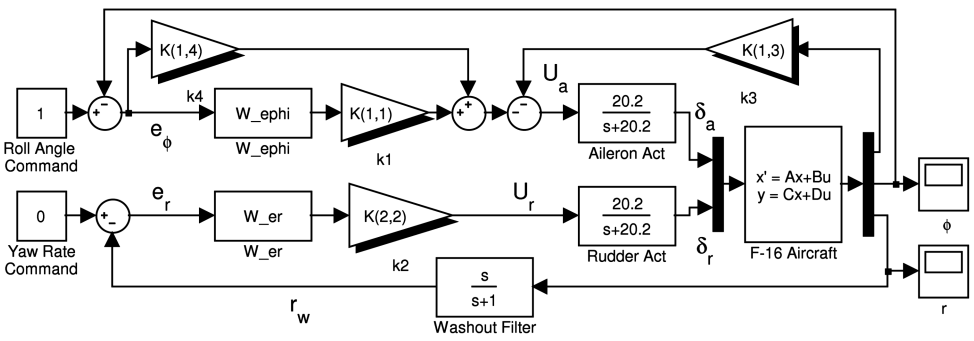

Fig. 3 Wing-leveler lateral control system for the F-16.

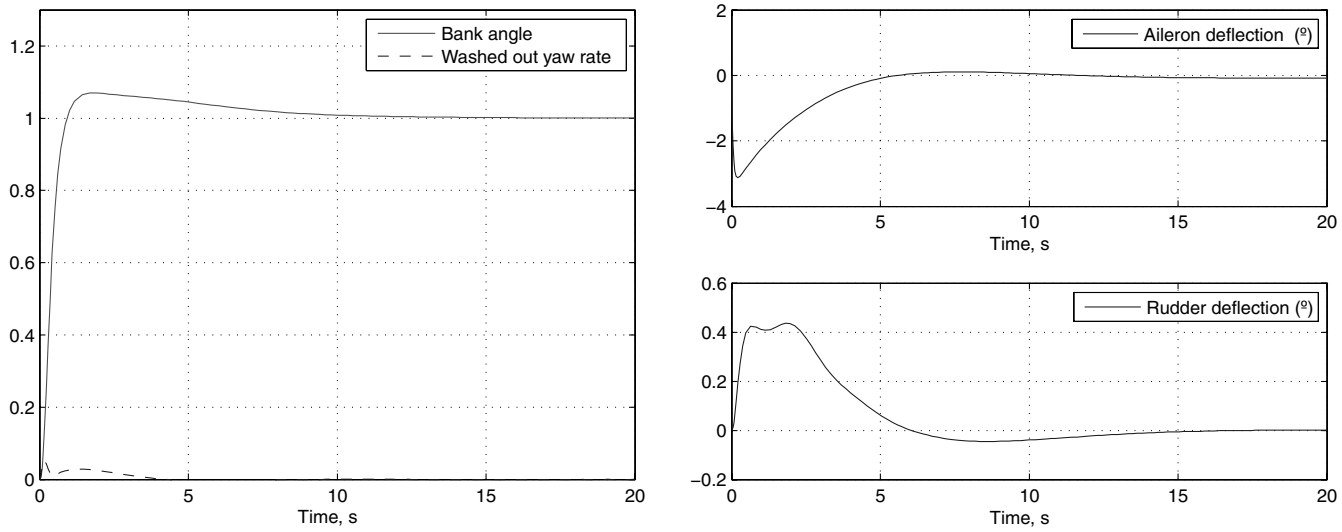

Fig. 4 Time response and actuator effort (first LTI design, K_1 controller).

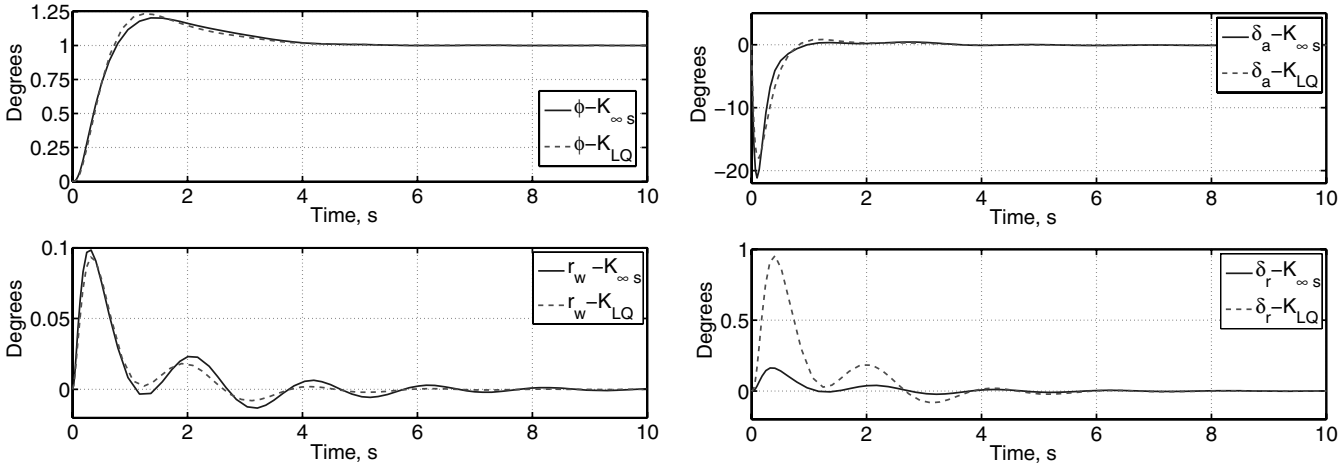

Fig. 5 Time response and actuator effort (second LTI design, $K_{\infty s} = K_2$ controller compared with K_{LQ} in [16]). Here, δ_a and δ_r are the aileron and rudder deflections, respectively, ϕ is the bank angle, and r_w is the washed out yaw rate.

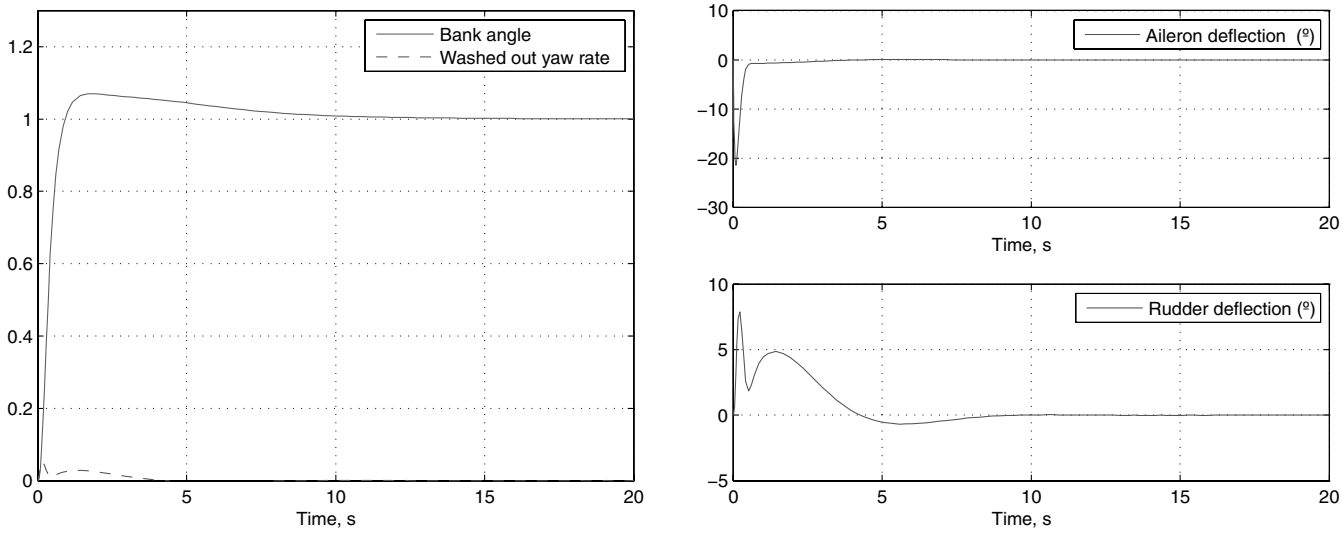

Fig. 6 Time response and actuator effort (third LTI design, K_3 controller).

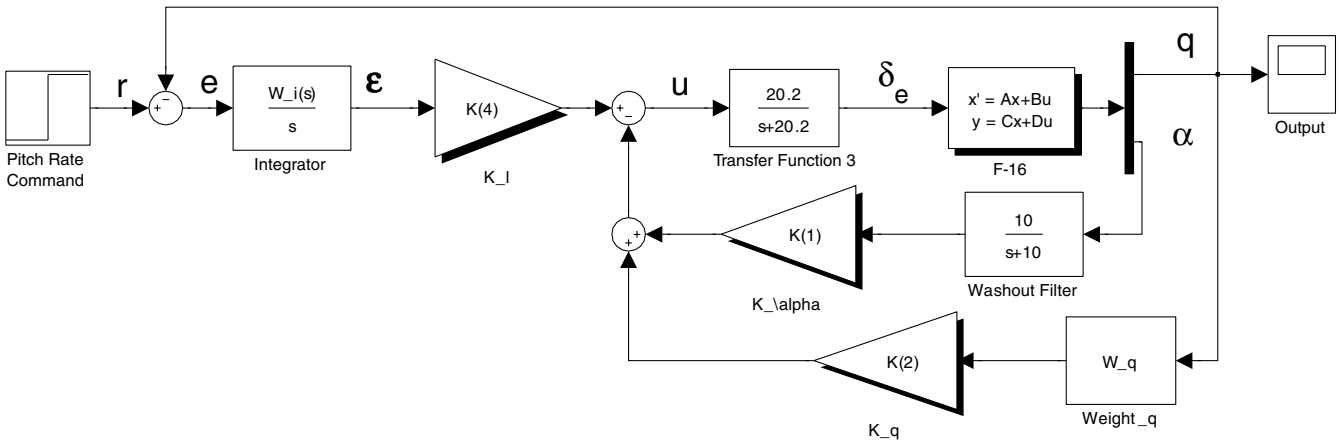

Fig. 7 Block diagram of the pitch-rate control system for the F-16.

The time response is presented in Fig. 5 and compared with the one in Kureemun and Bates [16]. In this case, our result is slightly better, and the robustness margin after the optimization is $\gamma_\star = 3$.

3) Another way of improving the performance is as follows. In the first example, the controller bounds have not been reached; therefore, a significant improvement in performance could be made by simply increasing the first controller's gain until the aileron deflection is 22 deg. In this case, $K_3 = 9 \times K_1$ produces a much faster time response with less overshoot (see Fig. 6), and the aileron deflection is within the allowable upper bound. This can be considered as another way of changing the performance weights. Here, the performance has a similar response as the one achieved with a *dynamic* $\mathcal{H}_\infty$ controller in Kureemun and Bates [16], at the expense of a lower tolerance to uncertainty, that is, γ increases up to 105.

B. LPV Case: Pitch-Rate Control

In this subsection, we demonstrate the application of a LPV SOF controller for the pitch-rate control of the F-16 short-period approximation model. This model is obtained by linearizing the nonlinear F-16 model [17]. The states of the linearized model describing the longitudinal mode are the pitch rate q and the angle of attack α. Figure 7 shows the block diagram of the pitch-rate control system. The measured output for feedback is $y(t) = [\alpha_f \quad q \quad \epsilon]^T$, where α_f is the low-pass-filtered angle-of-attack signal and ϵ is the integrator output. The performance requirement in this example is to track the pitch rate with the control input signal $u(t) = -K(\rho)y(t)$, where the SOF LPV controller $K(\rho)$ is designed using Lemma 3. The augmented LPV model $G_s(\rho)$ is constructed with the following weighting function:

$$W(s) = \begin{bmatrix} \frac{W_i}{s} & 0 \\ 0 & W_q \end{bmatrix} = \begin{bmatrix} \frac{100}{s} & 0 \\ 0 & 25 \end{bmatrix}$$

Parameter ρ varies in a rectangle defined by height $h \in [0; 16,000]$ m and true airspeed $V_{\text{tas}} \in [300, 502]$ ft/s. The F-16 aircraft with c.g. position $X_{\text{cg}} = 0.3\bar{c}$ is trimmed under the conditions shown in Table 1. These conditions follow the flight trajectory mentioned in Stevens and Lewis [17], p. 352. The duration of the operation of each model and the corresponding controller are also shown in the same Table. The system matrices for all flight conditions are presented in the Appendix. The resulting robustness margin for the designed controller $K(\rho)$ is $\gamma_\star = 5.75$.

From Fig. 8 it can be seen that the pitch-rate response closely follows the pitch-up command from $t_0 = 10$ s to $t_f = 20$ s. The pitch-up command brings the aircraft to a vertical position while decreasing the V_{tas} from 502 to 300 ft/s. The decrease in the true airspeed is due to the fact that no thrust input is considered in the linearized modeling equations. Thus, the SOF LPV controller synthesized using our algorithm tracks the input command with some guaranteed robustness. It can be noticed in the results that there

Table 1 Trim conditions for the F-16 LPV models used

Number	Height, Kft	V_{tas}, ft/s	$\dot{\theta}$, deg /s	Time, s
1	0	502	0	[0–10)
2	0	502	8.65	(10–20)
3	3.550	502	0	(20–35)
4	10	400	0	(35–50)
5	10	300	10	(50–62)
6	11	380	10	(62–70)
7	16	300	10	(70–80]

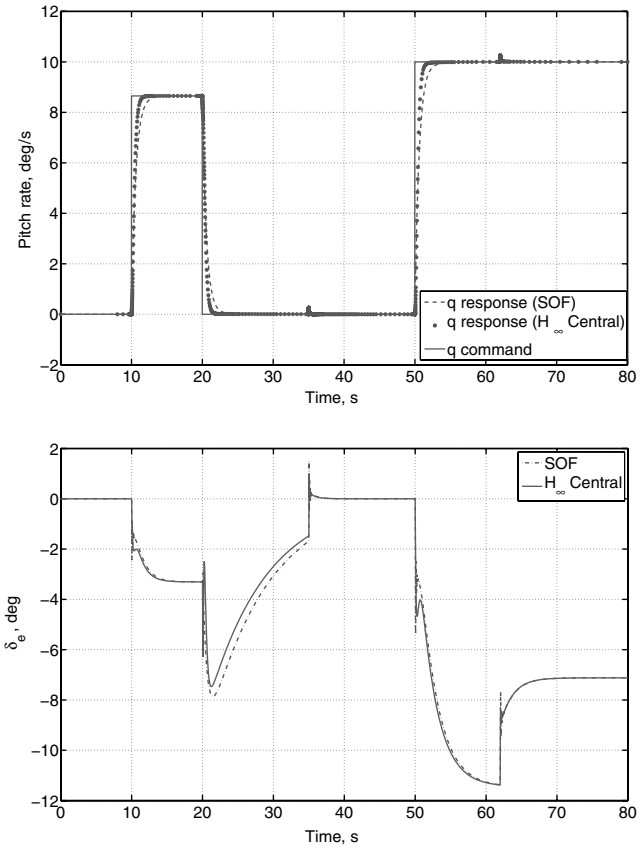

Fig. 8 Time response and elevator deflection of the pitch-rate command using the SOF LPV and dynamic LTI $\mathcal{H}_\infty$ controls.

exist high-frequency transients during the automated gain-scheduling process due to the fact that the commanded transitions among each working point are not smooth. Also, due to the mismatch in the state conditions in the simulation, at $t = 35$ and 62 s, some small transients appear due to the transition between vertices of the LPV model (see Table 1).

A dynamic LTI $\mathcal{H}_\infty$ controller $K(s)$ was also designed for the same F-16 model at trim condition number 4, as specified in Table 1. The robustness margin for this controller is $\gamma = 2.28$, but is valid only for flight condition number 4, not for the whole flight envelope. Both the LPV SOF and the LTI dynamic controllers were used for the whole flight trajectory and can be seen in Fig. 8. The latter provides a similar time response, but at the expense of a higher-order controller (5) and no guarantees of stability during the parameter transitions.

V. Conclusions

The main contribution of this work is the design of static LPV controllers that can guarantee both performance and robustness by solving a finite set of LMIs. The SOF controller design method also provides a procedure to integrate pole location specifications and a fixed controller structure in the design, which has a significant importance in aircraft applications. Finally the performance and robustness metric is improved by means of a simple iterative algorithm. Promising results were obtained when this design methodology was applied to a practical multiloop flight controller for the F-16 with an output feedback structure, which is traditionally employed in stability augmentation systems.

Appendix: Example System Matrices

I. LTI Model Description

The model is obtained from example 5.5-4 of Stevens and Lewis [17]. The trimming conditions chosen for this case are true airspeed $V_{\text{tas}} = 502$ ft/s, 300 psf dynamic pressure, and c.g. at $0.35\bar{c}$. The augmented model $G(s)$ with F-16 dynamics, washout filter, actuator dynamics, and the weighting functions is given in state-space form as

$$\dot{x}(t) = Ax(t) + Bu(t) + Gr_c, \quad y(t) = Cx(t) + Fr_c, \quad z(t) = Hx(t)$$

where the state vector is

$$x = [\beta \quad \phi \quad p \quad r \quad \delta_a \quad \delta_r \quad x_w \quad \epsilon]^T$$

the output vector is $y = [\epsilon \quad e_r \quad p \quad e_\phi]^T$, the performance output is $x = [\phi \quad r_w]^T$, and the corresponding state-space matrices are given as follows:

$$A = \begin{bmatrix} -0.3220 & 0.0640 & 0.0364 & -0.9917 & 0.0003 & 0.0008 & 0 & 0 \\ 0 & 0 & 1 & 0.0037 & 0 & 0 & 0 & 0 \\ -30.6492 & 0 & -3.6784 & 0.6646 & -0.7333 & 0.1315 & 0 & 0 \\ 8.5395 & 0 & -0.0254 & -0.4764 & -0.0319 & -0.0620 & 0 & 0 \\ 0 & 0 & 0 & 0 & -20.2 & 0 & 0 & 0 \\ 0 & 0 & 0 & 0 & 0 & -20.2 & 0 & 0 \\ 0 & 0 & 0 & 57.2958 & 0 & 0 & -1 & 0 \\ 0 & -1 & 0 & 0 & 0 & 0 & 0 & 0 \end{bmatrix}, \quad B = \begin{bmatrix} 0 & 0 & 0 & 0 & 20.2 & 0 & 0 & 0 \\ 0 & 0 & 0 & 0 & 0 & 20.2 & 0 & 0 \end{bmatrix}^T$$

$$C = \begin{bmatrix} 0 & 0 & 0 & 0 & 0 & 0 & 0 & 1 \\ 0 & 0 & 0 & -57.2958 & 0 & 0 & 1 & 0 \\ 0 & 0 & 1 & 0 & 0 & 0 & 0 & 0 \\ 0 & -1 & 0 & 0 & 0 & 0 & 0 & 0 \end{bmatrix}, \quad G = \begin{bmatrix} 0 & 0 & 0 & 0 & 0 & 0 & 0 & 0 \\ 0 & 0 & 0 & 0 & 0 & 0 & 0 & 1 \end{bmatrix}^T$$

$$H = \begin{bmatrix} 0 & 1 & 0 & 0 & 0 & 0 & 0 & 0 \\ 0 & 0 & 0 & 57.2958 & 0 & 0 & -1 & 0 \end{bmatrix}^T, \quad F = \begin{bmatrix} 0 & 1 & 0 & 0 \\ 0 & 0 & 0 & 1 \end{bmatrix}^T$$

II. LPV Model Description

Here, we provide the seven transfer functions obtained by short-period approximation of the F-16 linearized model under the conditions provided by Table 1. These transfer functions are used at each vertex of the convex polytope created for the SOF LPV controller design and implementation.

$$\begin{bmatrix} q \\ \alpha \end{bmatrix}_1 = \frac{\left[\frac{-10.452(s+0.989)}{-0.123(s+78.14)}\right]}{s^2 + 2.405s + 3.673}[\delta_e],$$

$$\begin{bmatrix} q \\ \alpha \end{bmatrix}_2 = \frac{\left[\frac{-10.536(s+1.07)}{-0.124(s+78.07)}\right]}{(s + 0.2285)(s + 2.407)}[\delta_e],$$

$$\begin{bmatrix} q \\ \alpha \end{bmatrix}_3 = \frac{\left[\frac{-9.408(s+0.891)}{-0.111(s+78.63)}\right]}{s^2 + 2.169s + 3.205}[\delta_e],$$

$$\begin{bmatrix} q \\ \alpha \end{bmatrix}_4 = \frac{\left[\frac{-4.897(s+0.577)}{-0.073(s+62.09)}\right]}{s^2 + 1.458s + 2.014}[\delta_e],$$

$$\begin{bmatrix} q \\ \alpha \end{bmatrix}_5 = \frac{\left[\frac{-2.360(s+0.121)}{-0.037(s+60.01)}\right]}{s^2 + 0.763s + 1.696}[\delta_e],$$

$$\begin{bmatrix} q \\ \alpha \end{bmatrix}_6 = \frac{\left[\frac{-4.462(s+0.4293)}{-0.059(s+71.14)}\right]}{s^2 + 1.27s + 2.195}[\delta_e],$$

$$\begin{bmatrix} q \\ \alpha \end{bmatrix}_7 = \frac{\left[\frac{-2.360(s+0.121)}{-0.037(s+60.01)}\right]}{s^2 + 0.763s + 1.696}[\delta_e]$$

Acknowledgments

The first author was partially supported by the Research Commission of the Generalitat de Catalunya (ref. 2005SGR00537) and CICYT Project No. DPI2005-04722. All authors appreciate the financial support of Zona Technology, Inc., and the reviewer's constructive comments.

References

[1] Gahinet, P., and Apkarian, P., "A Convex Characterization of Gain-Scheduled $\mathcal{H}_\infty$ Controllers," *IEEE Transactions on Automatic Control*, Vol. 40, No. 5, May 1995, pp. 853–864. doi:10.1109/9.384219

[2] Becker, G. S., and Packard, A., "Robust Performance of LPV Systems Using Parametrically-Dependent Linear Feedback," *Systems and Control Letters*, Vol. 23, No. 3, Sept. 1994, pp. 205–215. doi:10.1016/0167-6911(94)90006-X

[3] Scherer, C., "LPV Control and Full Block Multipliers," *Automatica*, Vol. 37, No. 3, March 2001, pp. 361–375. doi:10.1016/S0005-1098(00)00176-X

[4] Baldelli, D., Lee, D., Sánchez-Peña, R., Hopper, D., and Cannon, B., "Practical Modeling, Control and Simulation of an Aeroelastic Morphing UAV," *48th Structures, Structural Dynamics, and Materials Conference, AIAA/ASME/ASCE/AHS/ASC*, AIAA, Reston, VA, April 2007, pp. 1–19; also AIAA Paper 2007-2236.

[5] Blondel, V., and Tsitsiklis, J., "NP-Hardness of Some Linear Control Design Problems," *SIAM Journal on Control and Optimization*, Vol. 35, No. 6, 1997, pp. 2118–2127. doi:10.1137/S0363012994272630

[6] Syrmos, V., Abdallah, C., and Dorato, P., "Static Output Feedback: A Survey," *Proceedings of the 33rd IEEE Conference*, Vol. 1, Inst. of Electrical and Electronics Engineers, New York, Dec. 1994, pp. 837–842. doi: 10.1109/CDC.1994.410963

[7] Burke, J. V., Lewis, A., and Overton, M., "Stabilization via Nonsmooth, Nonconvex Optimization," *IEEE Transactions on Automatic Control*, Vol. 51, No. 11, Nov. 2006, pp. 1760–1769. doi:10.1109/TAC.2006.884944

[8] Gadewadikar, J., Lewis, F., and Abu-Khalaf, M., "Necessary and Sufficient Conditions for $\mathcal{H}_\infty$ Static Output-Feedback Control," *Journal of Guidance, Control, and Dynamics*, Vol. 29, No. 4, June 2006, pp. 915–920. doi:10.2514/1.16794

[9] Gadewadikar, J., Lewis, F., Xie, L., Kucera, V., and Abu-Khalaf, M., "Parameterization of All Stabilizing $\mathcal{H}_\infty$ Static State-Feedback Gains: Application to Output-Feedback Design," *Automatica*, Vol. 43, No. 9, Sept. 2007, pp. 1597–1604. doi:10.1016/j.automatica.2007.02.005

[10] Prempain, E., and Postlethwaite, I., "Static $\mathcal{H}_\infty$ Loop Shaping Control of a Fly-by-Wire Helicopter," *Automatica*, Vol. 41, No. 9, Sept. 2005, pp. 1517–1528. doi:10.1016/j.automatica.2005.04.001

[11] McFarlane, D., and Glover, K., "A Loop-Shaping Design Procedure Using $\mathcal{H}_\infty$ Synthesis," *IEEE Transactions on Automatic Control*, Vol. 37, No. 6, June 1992, pp. 759–769. doi:10.1109/9.256330

[12] Vinnicombe, G., *Uncertainty and Feedback: $\mathcal{H}_\infty$ Loop Shaping and the ν-Gap Metric*, Imperial College Press, London, 2001.

[13] Ghersin, A. S., and Sánchez-Peña, R. S., "LPV Control of a 6 DOF Vehicle," *IEEE Transactions on Control Systems Technology*, Vol. 10, No. 6, Nov. 2002, pp. 883–887. doi:10.1109/TCST.2002.804123

[14] Skelton, R., Iwasaki, T., and Grigoriadis, K., *A Unified Algebraic Approach to Linear Control Design*, Taylor and Francis, London, 1998.

[15] Glover, K., and McFarlane, D., "Robust Stabilization of Normalized Coprime Factor Plant Descriptions with ϵ-Bounded Uncertainty," *IEEE Transactions on Automatic Control*, Vol. 34, No. 8, Aug. 1989, pp. 821–830. doi:10.1109/9.29424

[16] Kureemun, R., and Bates, D., "Aircraft Flight Controls Design Using Constrained Output Feedback: A$\mathcal{H}_\infty$ Loopshaping Approach," AIAA Paper 2001-4281, 2001.

[17] Stevens, B., and Lewis, F., *Aircraft Control and Simulation*, Wiley, New York, 2003.

[18] Chilali, M., and Gahinet, P., "$\mathcal{H}_\infty$ Control Design with Pole Placement Constraints: An LMI Approach," *IEEE Transactions on Automatic Control*, Vol. 41, No. 3, March 1996, pp. 358–367. doi:10.1109/9.486637

[19] Xie, W., and Eisaka, T., "Design of LPV Control Systems Based on Youla Parameterization," *IEE Proceedings Control Theory & Applications* , Vol. 151, No. 4, 2004, pp. 465–472.

[20] Xie, W., and Eisaka, T., "Generalized Internal Model Architecture For Linear Parameter Varying Systems," *Proceedings of the 17th International Symposium on Mathematical Theory of Networks and Systems*, Paper FrPo3.2, July 2006, pp. 2590–2595.

[21] Li, L., and Paganini, F., "Structured Coprime Factor Model Reduction Based on LMIs," *Automatica*, Vol. 41, No. 1, Jan. 2005, pp. 145–151. doi:10.1016/S0005-1098(04)00247-X